Journal of Hydrology 541 (2016) 206–217

Contents lists available at ScienceDirect

Journal of Hydrology

journal homepage: www.elsevier.com/locate/jhydrol

Initial soil moisture effects on flash flood generation – A comparison between basins of contrasting hydro-climatic conditions

M.G. Grillakis [a], A.G. Koutroulis [a], J. Komma [b], I.K. Tsanis [a,c,*], W. Wagner [d], G. Blöschl [b]

[a] Water Resources Management and Coastal Engineering Laboratory, School of Environmental Engineering, Technical University of Crete, Greece
[b] Institute of Hydraulic Engineering and Water Resources Management, Vienna University of Technology, Austria
[c] Department of Civil Engineering, McMaster University, Hamilton, ON L8S 4L7, Canada
[d] Department for Geodesy and Geoinformation, Technische Unversität Wien, Austria

ARTICLE INFO

Article history:
Available online 21 March 2016

Keywords:
Initial soil moisture
Soil water index
Flood generation
Crete
Austria

SUMMARY

The purpose of this paper is to contribute to the understanding of the importance of the initial soil moisture state for flash flood magnitudes. Four extreme events that occurred in different case study regions were analysed, one winter and one autumn flash flood in the Giofiros and Almirida catchments in Crete, and two summer floods in the Rastenberg catchment in Austria. The hydrological processes were simulated by the spatially distributed flash flood model Kampus. For the Crete cases Kampus model was calibrated against remotely sensed soil moisture while for the Austrian case the model was calibrated against observed runoff. Kampus model was then used to estimate the sensitivity of the stream flow peak to initial soil moisture. The largest of the events analysed (in terms of specific peak discharge) was found to have a sensitivity of less than 0.2% flood peak change per % soil moisture change while the smallest event had a sensitivity of more than 3% flood peak change per % soil moisture change. This suggests that initial soil moisture effects on the flash flood response probably depend on event magnitude rather than on the climate or region. Moreover, the Austrian catchment was found to exhibit a more nonlinear relationship between antecedent soil moisture and the peak discharge than the Cretan catchments which was explained by differences in the soil type.

1. Introduction

Europe has experienced numerous catastrophic flash floods in the last decades with vast social and economic impacts on the affected areas (Hall et al., 2013; Merz et al., 2014). The frequency and the magnitude of the flash flood events have differed between Continental and Mediterranean regions in Europe, with a tendency of the latter to produce more extreme floods (Gaume et al., 2009; Norbiato et al., 2009).

There are a number of factors that affect the severity of floods including precipitation intensity, percentage of sealed catchment area, soil permeability, water holding capacity, topographic slopes and soil moisture content soil at the beginning of the event. In contrast to the other characteristics that do not change much between events, soil moisture can vary significantly, even on a sub daily time scale. Soil moisture can vary from near to the wilting point to saturation. It is considered as the most important soil factor for rapid runoff and flash flooding. Saturated soils obstruct precipitation to infiltrate, resulting in higher runoff regardless other environmental conditions. Soil moisture can, in fact, control whether a given rainstorm produces a major flash flood or not, due to the non-linear nature of runoff response to rainfall (Hlavcova et al., 2005; Komma et al., 2007; Zehe and Blöschl, 2004). In the framework of flood warning systems, the knowledge of soil moisture is crucial (Georgakakos, 2006; Javelle et al., 2010; Lacava et al., 2005; Raynaud et al., 2015; Van Steenbergen and Willems, 2013). Hence, it is essential to capture antecedent soil moisture well for flood forecasting applications (Berthet et al., 2009; Yatheendradas et al., 2008).

Michele and Salvadori (2002) evaluated the influence of antecedent soil moisture conditions on the flood frequency distribution based on derived distribution theory. Based on an analysis of soil moisture from point (in-situ) to footprint (remote sensing) scale (Joshi et al., 2011) concluded that soil properties and topography are the most significant physical parameters that jointly control the spatio-temporal evolution of soil moisture. In a similar study on an experimental catchment, (Nasta et al., 2013) found that, during wet periods, catchment topography is an important factor of

* Corresponding author at: Polytechioupolis, Kounoupidiana, Chania 73100, Greece.
E-mail address: tsanis@hydromech.gr (I.K. Tsanis).

http://dx.doi.org/10.1016/j.jhydrol.2016.03.007
0022-1694/

spatial soil moisture distribution whereas, during dry periods, it depend primarily on soil hydraulic properties. This is consistent with the earlier findings of (Grayson et al., 1997) in the Tarrawarra catchment. Based on model simulation, (Yoo et al., 1998) found that, during the rainfall event, soil texture plays a greater role for the soil moisture evolution than rainfall variability although this finding may be contingent on their particular catchment conditions (Viglione et al., 2010).

In order to assess soil moisture effects on flood magnitudes, soil moisture is needed at the catchment scale. However this is difficult to measure on an in-situ basis. An alternative is soil moisture retrieval by satellite sensors such as the series of passive multi-frequency radiometers (SMMR, Windsat, AMSR-E, etc. – see (de Jeu et al., 2008)) for which a long record of continuous measurements starting in 1978 is available, and the series of active microwave scatterometers, which begun with launch of the ERS 1scatterometerin 1991 (Naeimi et al., 2009; Wagner et al., 1999). The Advanced Scatterometer (ASCAT) started in 2007 (MetOp-A and MetOp-B) and continues to operate to date (Bartalis et al., 2007).

This paper investigates the importance of initial soil moisture for the flood magnitude in catchments of different geomorphology and hydro-meteorological regimes by making use of satellite-retrieved soil moisture and hydrological modelling.

2. Methodology

2.1. ERS scatterometer soil moisture data

The ERS scatterometer data used here allow the retrieval of surface soil moisture information on the top 2 cm soil layer (Parajka et al., 2006). The top layer of hydrological models, however, is usually considered to be the root zone which is much deeper than the satellite beam can penetrate. A transformation of the ERS data was hence used to account for the time delay as the water infiltrates from the surface into the soil based on a simple linear filter in the time domain (Wagner, 1998). In this method, soil water index (SWI) that should reflect root zone soil moisture is defined:

$$\mathrm{SWI}\ (t) = \frac{\sum_i m_s(t_i) e^{\frac{t-t_i}{T}}}{\sum_i e^{\frac{t-t_i}{T}}} \quad \text{for } t_i \leqslant t \tag{1}$$

where m_s is the surface soil moisture estimate from the ERS Scatterometer at time t_i and T is the time constant of the filter. T is related to the hydraulic characteristics of the top soil with more permeable soils being associated with smaller T because of the faster infiltration. However, at the pixel scale, this relationship is difficult to identify based on soil characteristics and can best be obtained by backcalculation from terrestrial soil moisture data and/or hydrological models (Parajka et al., 2009; Wagner, 1998). The SWI is calculated if there are at least one ERS Scatterometer measurement in the time interval $[t, t-T]$ and at least three measurements in the interval $[t, t-5T]$. Following (Brocca et al., 2012, 2010; Wagner, 1998; Wagner et al., 1999) a time constant of $T = 20$ days is well suited for the present application.

2.2. The hydrological model Kampus

The Kampus model used in this study is a spatially-distributed continuous rainfall–runoff model (Bloschl et al., 2008; Viglione et al., 2010). Kampus model uses a 15 min time step and consists of a snow routine, a soil moisture routine and a flow routing routine. The snow routine represents snow accumulation and melt by the degree-day concept. The soil moisture accounting routine is the main part controlling runoff formation. It represents the runoff generation and changes in the soil moisture state of the catchment and involves three parameters: the maximum soil moisture storage L_s, a parameter representing the soil moisture state above which evaporation is at its potential rate, termed the limit for potential evaporation L_P, and a parameter in the non-linear function relating runoff generation to the soil moisture state, termed the non-linearity parameter β. Runoff routing on the hillslopes is represented by an upper and two lower soil reservoirs. Excess rainfall Q_p enters the upper zone reservoir and leaves this reservoir through three paths, outflow from the reservoir based on a fast storage coefficient k_1; percolation to the lower zones with a percolation rate c_P; and, if a threshold of the storage state L_1 is exceeded, through an additional outlet based on a very fast storage coefficient k_0. Water leaves the lower zones based on the slow storage coefficients k_2 and k_3. Bypass flow Q_{by} is accounted for by recharging the lower zone reservoir (k_2) directly by a fraction of the excess rainfall. k_1 and k_2 as well as c_P have been related to the soil moisture state in a linear way. The outflow from the reservoirs represents the total runoff Q_t on the hillslope scale. These processes are represented on a 1 km × 1 km grid. Kampus model states for each grid element are the snow water equivalent, soil moisture S_s of the top soil layer, the storage of the soil reservoirs S_1, S_2, S_3 associated with the storage coefficients k_1, k_2, k_3, with $k_1 < k_2 < k_3$.

In the soil moisture routine, the sum of rain and melt, $P_r + M$, is split into a component dS that increases soil moisture of a top layer, S_s, and a component Q_p that contributes to runoff. The components are split as a function of S_s:

$$Q_p = \left(\frac{S_s}{L_s}\right)^{\beta} \cdot (P_r + M) \tag{2}$$

L_s is the maximum soil moisture storage, β controls the characteristics of runoff generation and is termed the non-linearity parameter. If the top soil layer is saturated, i.e., $S_s = L_s$, all rainfall and snowmelt contributes to runoff and dS is 0. If the top soil layer is not saturated, i.e., $S_s < L_s$, rainfall and snowmelt contribute to runoff as well as to increasing S_s through $dS > 0$:

$$\begin{aligned} dS &= P_r + M - Q_p - Q_{by} && \text{if } \ P_r + M - Q_p - Q_{by} > 0 \\ dS &= 0 && \text{otherwise} \end{aligned} \tag{3}$$

where additionally, bypass flow Q_{by} is accounted for. The effect of the soil routine is that the contribution of precipitation to runoff is small when the soil is dry (low soil moisture values), while it becomes larger in wet soil conditions.

Analysis of the runoff data of the Rastenberg catchment indicated that flow that bypasses the soil matrix and directly contributes to the storage of the lower soil zone is important for intermediate soil moisture states S_s. For $\xi_1 \cdot L_s < S_s < \xi_2 \cdot L_s$ (with $\xi_1 = 0.4$, $\xi_2 = 0.9$) bypass flow was assumed to occur as:

$$\begin{aligned} Q_{by} &= \alpha_{by} \cdot (P_r + M) && \text{if } \ \alpha_{by} \cdot (P_r + M) < L_{by} \\ Q_{by} &= L_{by} && \text{otherwise} \end{aligned} \tag{4}$$

while no by pass flow was assumed to occur for dry and very wet soils. Changes in the soil moisture of the top soil layer S_s from time step $i-1$ to i are accounted for by

$$S_{s,i} = S_{s,i-1} + (dS - E_A) \cdot \Delta t \tag{5}$$

The only process that decreases S_s is evaporation E_A which is calculated from potential evaporation, E_P, by a piecewise linear function of the soil moisture of the top layer:

$$\begin{aligned} E_A &= E_P \cdot \tfrac{S_s}{L_p} && \text{if } \ S_s < L_p \\ E_A &= E_P && \text{otherwise} \end{aligned} \tag{6}$$

where L_p is a parameter termed the limit for potential evaporation. Potential evaporation was estimated by the modified Blaney–Criddle method as a function of air temperature.

The model has been used in numerous studies including (Grillakis et al., 2010) for analysis of the flash flood event that occurred in Slovenia on 18 September 2007.

3. Case study areas

3.1. Description of the case study catchments

The Giofiros catchment (Fig. 1) is a small (186 km^2) Mediterranean catchment located in the central part of Crete near Heraklion city (lat 35°12′, long 26°06′). The climate of the catchment is classified as Csa in the Köppen-Geiger climate classification (Peel et al., 2007) with warm dry summers and clement winters. Precipitation occurs mainly in the winter months between October and May. The average annual precipitation over the catchment ranges between 469 mm and 1217 mm with a mean of 827 mm over a 30 year record (1976–2005). The lower part of Giofiros catchment is relatively flat with smooth slopes while its upstream parts are steep. The soil is mainly alluvial and contains a relatively high percentage of clay, and some areas of rock. The geology consists of extensive strata of marly limestone, flysch and sandstone, gypsum and alluvial deposits. The major land use types are vineyards, olive trees and farmlands, which are also present along the stream banks. During the last two decades the northern parts of the basin near the outlet have been abruptly urbanised. The catchment exhibits seasonal flow, mainly during the wet period, typically between October and March (Ganoulis, 2003).

Almirida is a 24.7 km^2 catchment (Fig. 1) in the West of Crete near Chania (lat 35°26′ lon 24°12′). It exhibits moderate orography with elevation ranging between 0 and 527 m with a mean of 206 m. Almirida has the same climate as Giofiros basin. The average annual precipitation within the basin is 648.7 mm from a 32 year record (1975–2007). The runoff of the catchment is ephemeral and takes place only during rainfall events. Therefore, there is no gauging equipment installed. The catchment is mainly covered by scrub and natural grassland (42.3%), olive groves (36.6%) and agricultural land interrupted by wide areas of natural vegetation (20.6%), with as little as 0.6% urban fabric (Tsanis et al., 2013). The geology is mainly biogenic limestone, marl, clay and conglomerate, and crystalline limestones locally covered by marbles, medium crystalline, grey to black-grey, well-bedded in banks.

The Rastenberg catchment (Fig. 2) is located in northern Austria, approximately 120 km north-west of Vienna. At the Rastenberg stream gauge the catchment size is 96 km^2. Elevations range between 514 and 932 m. The catchment is drained by the Purzelkamp river which is a tributary to the Kamp river. The catchment is hilly with deeply incised channels. The geology of the catchment is mainly granite and gneiss. Weathering has produced sandy soils with a large storage capacity throughout the catchment. Approximately 50% of the catchment is forested and the rest is crop land and pasture. Mean annual precipitation is about 900 mm of which about 300 mm become runoff. During flood events, only a small proportion of rainfall contributes to runoff. Typically, the event runoff coefficients are 10% or less. As rainfall increases in magnitude, the runoff response characteristics change fundamentally because of the soil moisture changes in the catchment and the runoff coefficients can exceed 50% (Komma et al., 2007).

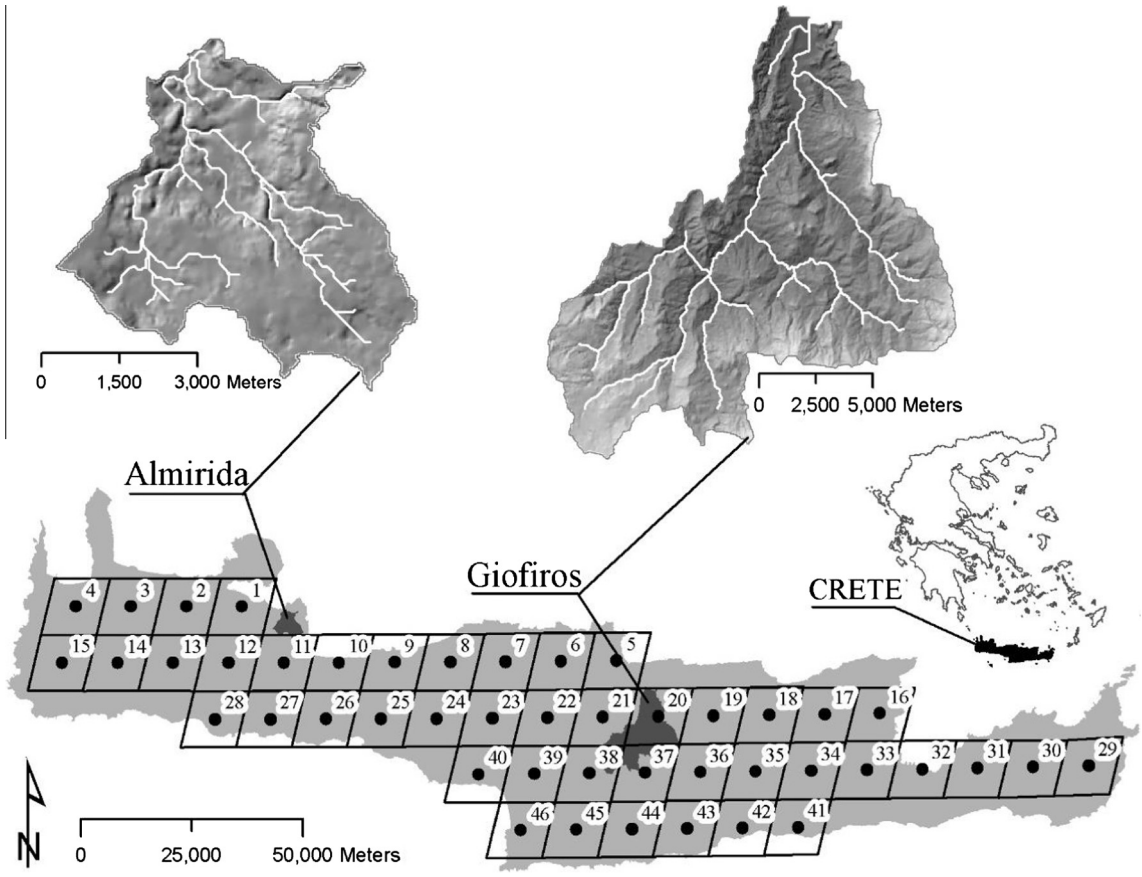

Fig. 1. Almirida and Giofiros river network (upper left and right) and catchment locations on the island of Crete (bottom). The ERS mesh on which the SWI was available for the island is also shown.

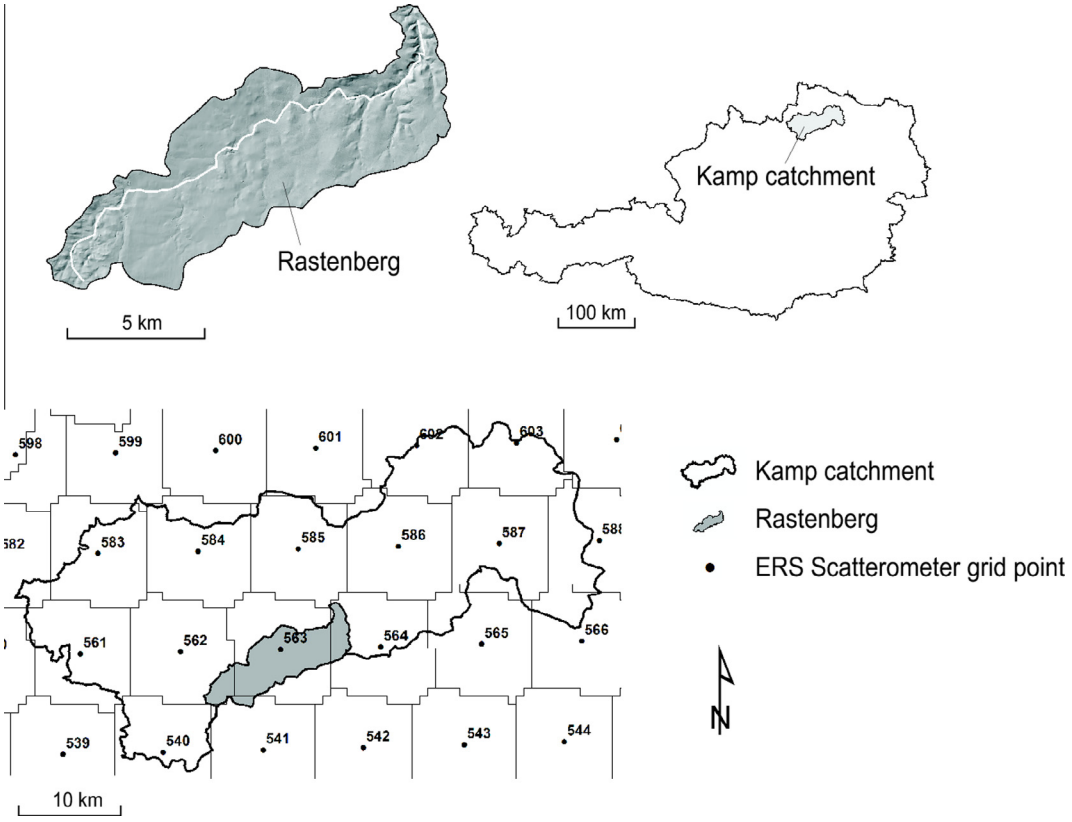

Fig. 2. Topography of Rastenberg catchment (top left) and Kamp catchment location in northern Austria (top right). The ERS scatterometer data are available for each cell in the bottom panel with the dots indicating the centroids.

3.2. Case study flash flood events

The Giofiros flood on the 13th of January 1994 was extraordinary both due to its total rainfall depth and its intensities. At noon of 13th January 1994, the intensity of the precipitation increased, reaching a maximum 5 h precipitation accumulation of 123 mm at 21:00. The rainfall eventually stopped at 24:00, after almost 9 h (Koutroulis and Tsanis, 2010). The total rainfall depth of the event for the 13th of January reached a maximum of 183 mm in the southern part of the basin (Agia Barbara rain gauge, 570 m elevation), which is very large compared to the mean annual precipitation of 827 mm. The maximum recorded intensity was 37 mm/h at the Agia Barbara rain gauge. The spatial distribution of the total precipitation of the event is shown in Fig. 3. There are three key features that contributed to the large magnitude of the damages. The soils have relatively poor infiltration capacities. Additionally, large areas with vineyard cultivation were ploughed in order to be renewed as the Phylloxera disease had affected the vines, which contributed to the poor soil condition. Finally, wooden debris accumulated in the river bed and decreased the transport capacity of the stream. The exact flood characteristics were not recorded due to stage gauge destruction at 20:00 during the flash flood. A detailed synoptic meteorological analysis of the event can be found in (Koutroulis and Tsanis, 2010) along with flow and hydraulic modelling reconstruction of the event.

The flash flood event in the Almirida catchment took place on the 17th of October of 2006. Before the event, no precipitation was recorded in a five month period apart from 21 mm on 11th and 12th of October. Even though the soils were very dry, the flood event was substantial. Early in the morning the rain started, delivering a total rainfall depth of 200 mm, recorded by a rain gauge

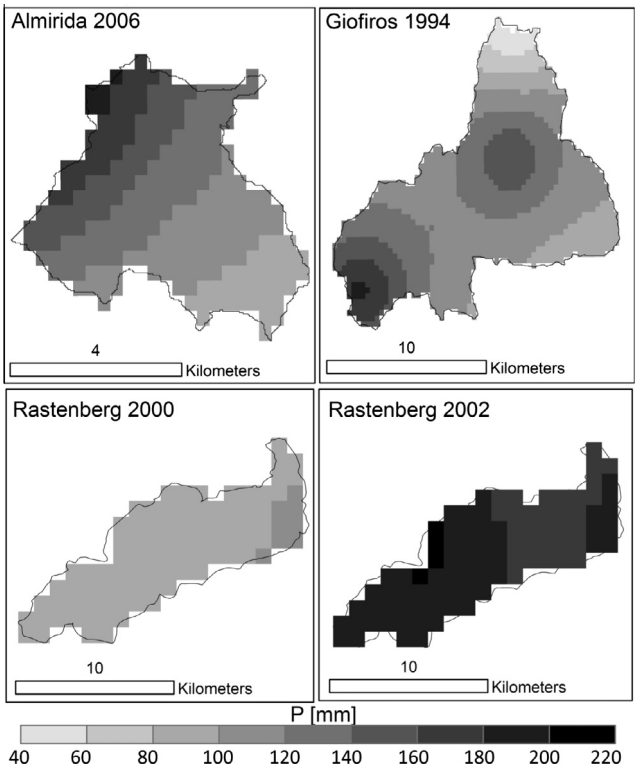

Fig. 3. Spatial distribution of the total precipitation for the analysed events.

1 km west of Almirida's catchment outlet. The total precipitation depth of the event is shown in Fig. 3. The storm was caused by a frontal depression that passed over the island of Crete. (Tsanis et al., 2013) report an approximate storm speed of 65 km h^{-1} estimated from High-resolution MeteoSat imagery, that classifying it as a potential Mediterranean tropical storm, a rather rare phenomenon (Lagouvardos et al., 1996). The peak rainfall took place at noon of 17th of October and a joint estimation using terrestrial and radar measurements showed that it was about 23.0 mm h^{-1} and lasted for about 30 min (Daliakopoulos and Tsanis, 2012). The precipitation resulted in an estimated peak discharge of 225 m^3 s^{-1}. A detailed post event field survey showed that the water depth of the stream near the outlet reached approximately 2 m. The discharge was estimated with the help of floodmarks (Gaume et al., 2009) and 1D/2D hydraulic modelling (Tsanis et al., 2013).

For the Austrian catchment of Rastenberg, two events were analysed. The first event is an extreme flood event that took place on 7th of August 2002. The average basin rainfall was estimated at about 200 mm over a time period of 42 h. The recorded peak discharge was 110 m^3/s, which is six times larger than the second largest observed peak in the 30 year record, causing enormous damage in the area (Merz and Blöschl, 2008a, 2008b). The second event analysed is a small event that occurred on 7th of August 2000. The total rainfall depth reached 23 mm with maximum intensities of 4 mm/15 min. Rainfall was highly localised so that over the catchment area of 96 km^2 the event peak was only 2.5 m^3/s. This event was included to the analysis in order to assess the temporal behaviour of soil moisture dynamics and the effect of antecedent soil moisture on event peak flow for a minor flood.

4. Results

4.1. Hydrological model calibration

For the two Cretan catchments ERS scatterometer data from 1992 to 2006 at a 25 km grid resolution were used (Fig. 1). From the ERS data SWI timeseries were estimated for each catchment. The Kampus model was calibrated for the Crete catchments in two steps. In a first step, a recursive optimisation scheme was used to calibrate the soil moisture controlling parameters S_s, L_s and β, against the SWI index for the period between October 1992 and July 1993. In the case of Almirida, data from nearby rain gauges was combined to the weather radar data of NSA Souda Bay C-Band radar to derive high temporal and spatial resolution precipitation fields (Daliakopoulos and Tsanis, 2012). The resulted gridded precipitation product was used to simulate the event, in combination with model parameter identification from the available land cover, soil and topographic data. The simulated hydrograph was used as an input to a 1D and a 2D hydraulic model (Tsanis et al., 2013). The simulations verified the maximum floodmark in specific control sections and the time of peak of the post event field survey data. In the case of Giofiros event, the precipitation was derived from IDW interpolation of high temporal resolution station data.

For the Austrian case study (Fig. 2), ERS scatterometer soil moisture estimates for the period October 1997 and October 2000 were used. Data accuracy was checked by a noise indicator (Bartalis et al., 2006; Naeimi et al., 2009). The model parameters were then identified based on the 'dominant processes concept' of (Grayson and Blöschl, 2001; Reszler et al., 2008) which suggests that, at different locations and different points in time, a small number of processes will dominate over the rest. Land use, soil type, landscape morphology (e.g. the degree of incision of streams) and information on soil moisture and water logging based on field surveys were used. The precipitation data were obtained from rain gauge data that were interpolated using the inverse distance approach. Discussions with locals provided information on flow pathways during past floods. Runoff simulations, stratified by time scale and hydrological situations, were compared with runoff data, and the simulated subsurface dynamics were compared with piezometric head data, both for the period 1993–2003. Due to the high amount of data, the SWI was used for validation rather than for calibration. The model was extensively tested against independent runoff data both at the seasonal and event scales for the period 2004–2006 (Blöschl, 2010).

4.2. Simulations results

Kampus model was designed to represent both runoff and catchment scale soil moisture well. Figs. 4 and 5 present the times series and scatter plots of simulated and satellite observed soil moisture, respectively. There are significant differences between the results obtained from the Cretan and Austrian catchments. As would be expected, in the Mediterranean climate of Crete soil moisture exhibits larger seasonality, due to the strong seasonality of the precipitation regime. The Rastenberg climate exhibits much smaller differences, as summer precipitation is slightly larger than winter precipitation. The catchment never dries out completely. It is interesting to note that there is a good agreement of simulated and satellite retrieved soil moisture (SWI) in the summer and autumn months in Rastenberg (Fig. 3, bottom) even though the satellite data were not used for parameter calibration.

The statistical characteristics of the soil moisture dynamics are given in Table 1. In Giofiros and Almirida there is very little bias as the mean simulated soil moisture and the mean SWI match within less than a percent. In Rastenberg, the mean simulated soil moisture is only slightly larger than the mean SWI. Similarly, the standard deviations of simulated soil moisture and SWI are consistent in all three catchments, indicating that SWI can capture the statistical characteristics of seasonal soil moisture variability very well for the events examined. In terms of the agreement between simulated soil moisture and SWI for a given point in time, the root mean squared errors are 6.6%, 10.3% and 12.7% for the Giofiros, Almirida and Rastenberg catchments, respectively. The differences are even more pronounced for the coefficient of determination, r^2, which is 0.82, 0.67 and 0.37 for the three catchments. Overall, the satellite data of the Crete case studies much better represent the seasonal dynamics of soil moisture than those of the Austrian catchment, mainly because of three reasons. First, the contrast between summer and winter in Crete is much larger than in Austria. Second, there are snow processes in Austria which confound the interpretation of the scatterometer soil moisture data. The days with snow cover have been excluded from Fig. 4, as the scatterometer data do not represent soil moisture when snow is on the ground. Third, the Rastenberg catchment is highly forested which can, again confound the satellite signal, while the Crete catchments have very little forest.

The results of the hydrological simulations of the events are shown in Figs. 5–8. Where available, the simulated soil moisture state before the event was validated against SWI. The values of SWI were 22% (Giofiros), 2.5% (Almirida) and 38% (Rastenberg, 2000 event). In all cases, the SWI represents the simulated soil moisture well in terms of RMSE. More specifically, in Fig. 5 is shown that the simulated soil moisture represents well the SWI, prior and after the flood, in the case of Giofiros event. It is interesting to note that the precipitation event, led to a 20% increase of the soil moisture, but due to its short duration it did not surpass the 50% of its field capacity. On the other hand for the Almirida event (Fig. 6) at the end of the summer, the soil moisture prior the event was very low, while it almost increased by 50% from the flash flood

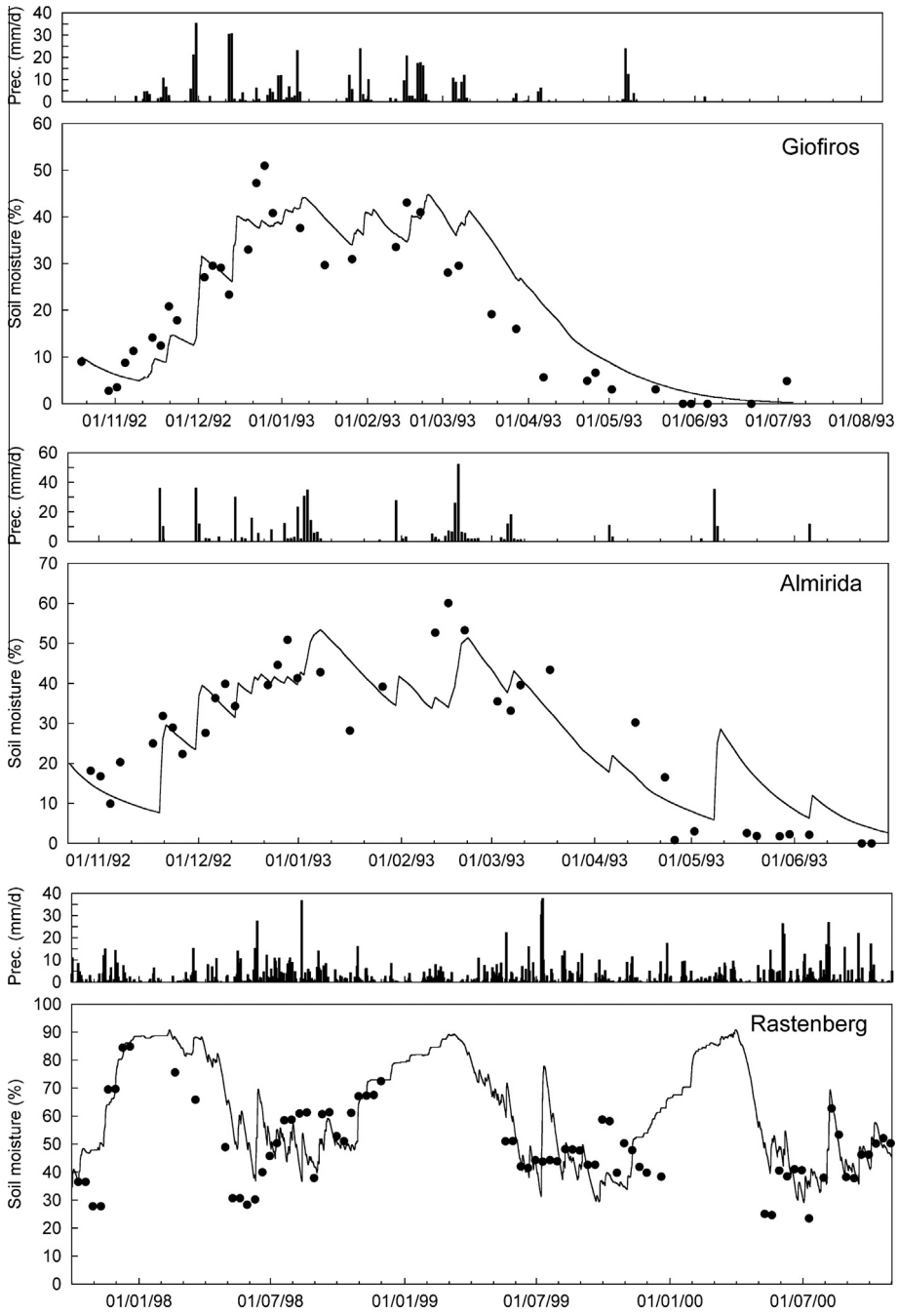

Fig. 4. Model simulated soil moisture (continuous line) and satellite based SWI index (dots) for Giofiros, Almirida and Rastenberg. In the latter, days with snow cover are excluded.

event. Due to the scarce ERS measurements, no SWI could be estimated after the flash flood event of Almirida. For the Rastenberg 2000 event (Fig. 7), the SWI verifies the simulated soil moisture series. The major precipitation event that caused the high flow of the event increased the soil moisture by 25%. In Fig. 8 the Rastenberg 2002 flood is presented. The precipitation event occurred in two phases. At the first phase, the soil moisture was increased from 50% to almost 85%. At the second phase, the precipitation cause a further increase in the soil moisture, increasing it to almost 100% by the end of the event. At that time, the peak discharge of 110 m^3/s. During the event, no SWI measurements were available to be compared to the simulated soil moisture.

4.3. Sensitivity analyses

In a next step, the effect of the initial soil moisture on peak discharges and on the soil moisture evolution during the events was examined. The initial soil moisture state was varied between 0% and 90%. The simulated soil moisture was compared to the SWI for the events of Giofiros and Rastenberg 2000 where SWI data were available. Fig. 9 (left panels) shows the results in terms of the goodness of fit (root mean squared error, RMSE) of the simulated soil moisture to the satellite based SWI during the periods shown in Figs. 5 and 7. As can be seen in Fig. 9 (dashed lines), the minimum RMSE was obtained for initial soil moisture between

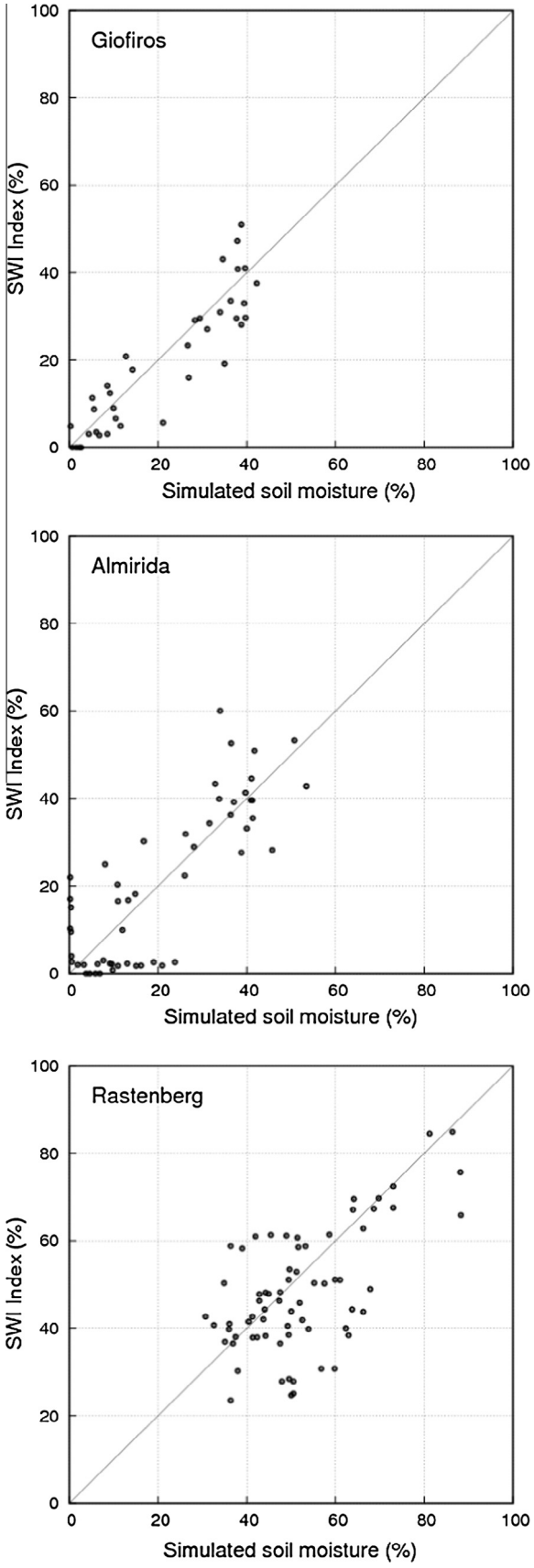

Fig. 5. Model simulated soil moisture (%) versus satellite based SWI index (%) for Giofiros, Almirida and Rastenberg (periods as of Fig. 3). In Rastenberg, days with snow cover are excluded.

Table 1
Characteristics of the seasonal soil moisture dynamics in the three catchments. The simulated soil moisture is S_s estimated by the hydrological model. SWI is the satellite based soil moisture estimate. Figs. 3 and 4 show details of the soil moisture dynamics.

Catchment	Giofiros		Almirida		Rastenberg	
Period	Oct. 1992–July 1993		Oct. 1992–June 1993		Oct. 1997–Oct. 2000	
	Simulated	SWI	Simulated	SWI	Simulated	SWI
Mean (%)	21.0	19.4	20.3	20.2	52.4	48.5
Stddev. (%)	14.9	15.3	16.0	18.0	13.3	14.1
RMSE (%)	6.6		10.3		12.7	
r^2	0.821		0.667		0.370	

20 and 30% in the case of the Giofiros event, and 50% for the Rastenberg 2000 event, respectively. These ranges are close to the soil moisture states actually used as initial conditions for the simulations. Additionally, the relative peak runoff (peak runoff of the sensitivity study divided by the observed peak runoff in percent) is shown as solid lines in the four panels, representing the sensitivities of peak runoff to the initial soil moisture.

There are major differences between the events. The effect of initial soil moisture on peak discharge is almost linear in the Cretan case study events (Fig. 9 – upper panels). In contrast, the effect of initial soil moisture on peak discharge is non-linear in the two Rastenberg events. The non-linearity is attributed to the sandy soil texture in the Rastenberg catchment. The initial losses in the catchment can reach up to 60 mm (Reszler et al., 2008) as most of the early event rainfall infiltrates. Once the storage capacity of the catchment is reached, runoff increases dramatically. Equally important to the non-linearity is the absolute value of the sensitivity of peak flow to initial soil moisture which is represented by the slope (Table 1 – bottom line) of the solid lines in Fig. 9. The lowest sensitivity occurs for the Almirida event. The specific peak flow of this flash flood was 5 $m^3/s/km^2$ which, by any standard, is enormous for a 25 km^2 catchment (Merz and Thieken, 2009). Clearly, this is the largest event, so the lowest sensitivity to soil moisture is not surprising. This is because essentially all the event rainfall becomes runoff since saturation is reached early in the event. The magnitude of the peak flow is hence no longer controlled by infiltration and runoff generation (since the runoff coefficient is close to unity) but by runoff routing (Viglione et al., 2009). The Giofiros and Rastenberg 2002 events were both very large floods (but not as large as the Almirida event). For these two events, the sensitivity is similar and ranges between about 0.2% and 1% flood peak change per % initial soil moisture change. The Rastenberg event in 2000 was rather small (the specific peak flow was 0.03 $m^3/s/km^2$ while it was 5 for the Almirida event). Not surprisingly, for the Rastenberg event in 2000 the sensitivity is much larger than for all the other events, ranging from 0.4 to about 3% flood peak change per % initial soil moisture change. Clearly, as the event magnitude decreases, the sensitivity of peak flows to initial soil moisture increases (see Table 2).

5. Discussion and conclusions

This paper analyses the effect of antecedent soil moisture on the magnitude of a few selected floods with extreme magnitudes. We examined this question by analysing two flood events in Crete and two events in Austria as case studies. The sensitivity analyses indicate that initial soil moisture is in all cases important for peak discharge but the magnitude of the effect depends on the magnitude of the event. The Almirida flood was very extreme indeed with a specific peak flow 5 $m^3/s/km^2$. For this event, the sensitivity of peak flow was always less than 0.2. However, for smaller events,

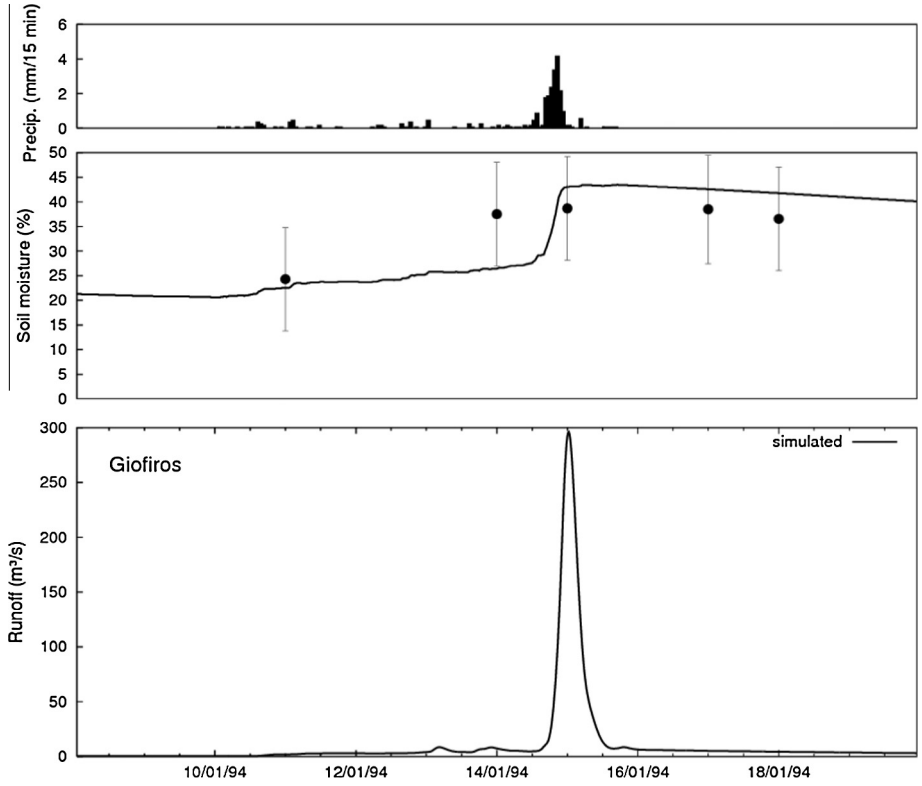

Fig. 6. Giofiros event precipitation (top), simulated soil moisture (centre – continuous line), satellite based SWI index (centre – dots), noise estimates of the SWI index (centre – error bars), and simulated event runoff (bottom).

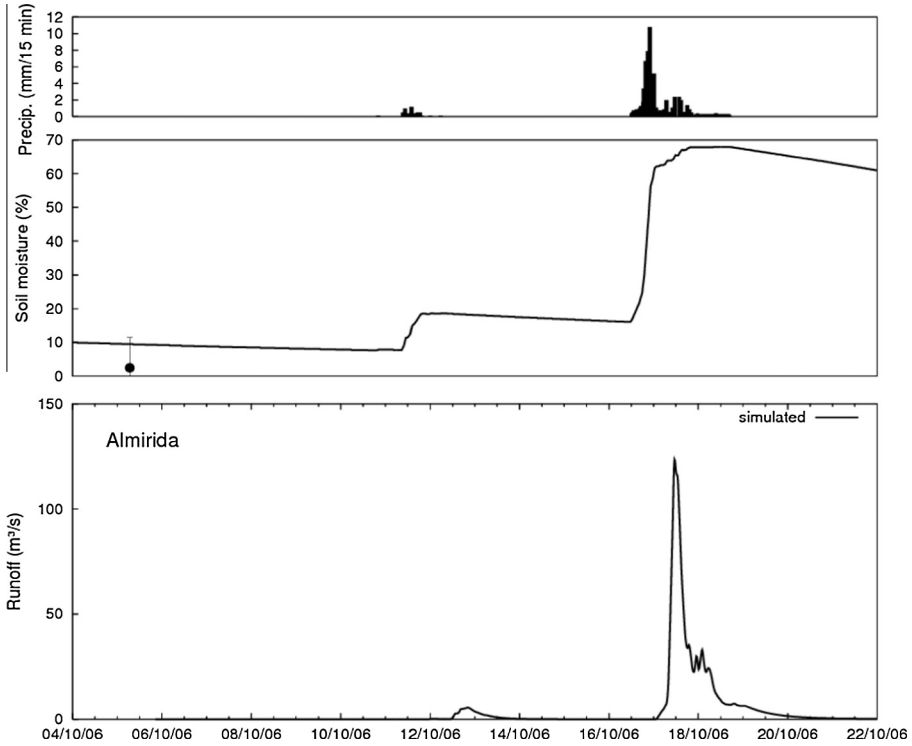

Fig. 7. Almirida event precipitation (top), simulated soil moisture (centre – continuous line), satellite based SWI index (centre – dot), noise estimates of the SWI index (centre – error bar), and simulated event runoff (bottom).

initial soil moisture becomes increasingly more important and can affect flood peaks by a factor of more than 2 in the Rastenberg 2000 example analysed here. This is fully consistent with hydrological reasoning as one would expect runoff generation to be more important for smaller events. This finding is very relevant for flash flood forecasting systems as accurate antecedent soil moisture

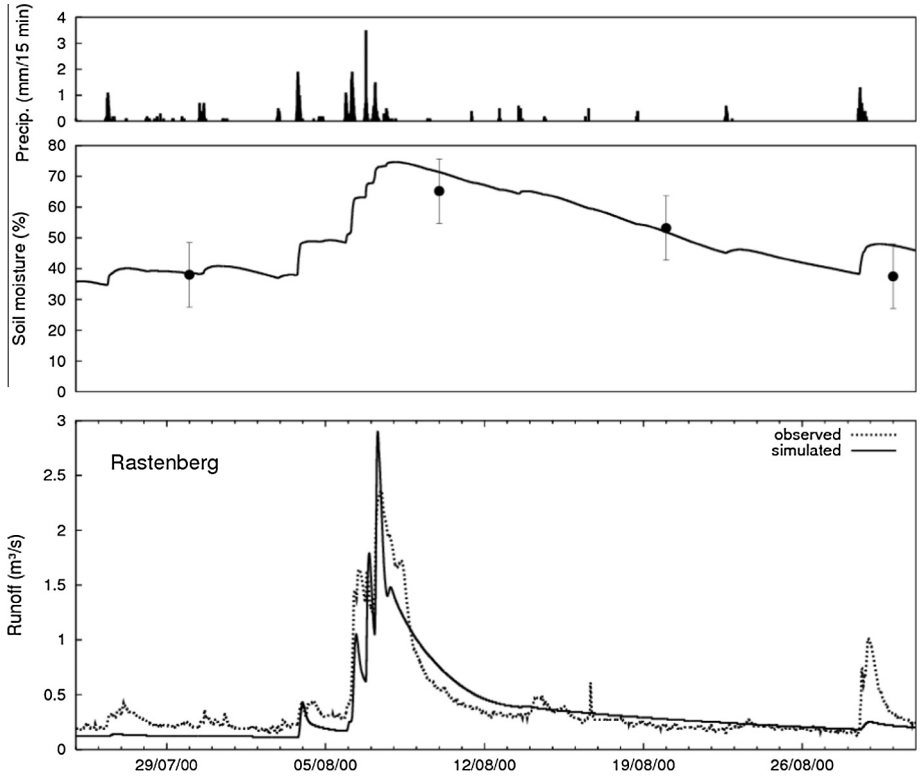

Fig. 8. 2000 flood event in Rastenberg. Event precipitation (top), simulated soil moisture (centre – continuous line), satellite based SWI index (centre – dots), noise estimates of the SWI index (centre – error bars), observed event runoff (bottom – dashed line) and simulated event runoff (bottom – solid line).

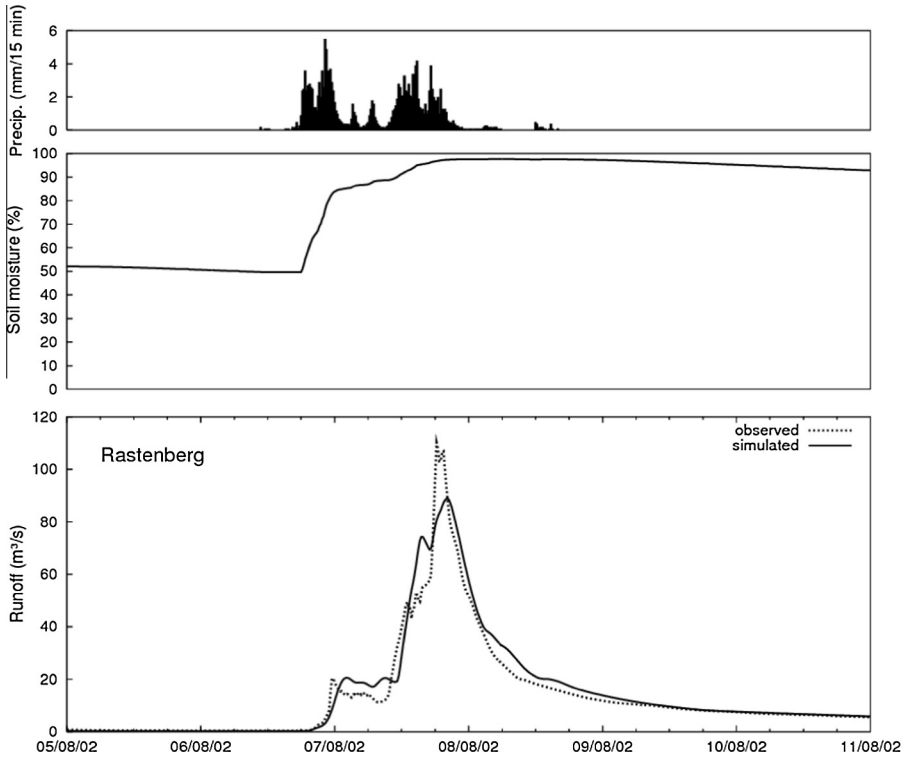

Fig. 9. 2002 flood event in Rastenberg. Event precipitation (top), simulated soil moisture (centre – continuous line), observed event runoff (bottom – dashed line) and simulated event runoff (bottom – solid line).

estimates may help avoid false alarms. Medium events usually contribute the most to the expected annual damage (Apel et al., 2006, 2004), so capturing them well is important. While the very extreme floods produce the largest damage, due to their scarcity, they do not contribute as much to the expected annual damage (see Fig. 10).

Table 2
Characteristics of the four flood events analysed in this paper. The sensitivity represents the % changes in the flood peak per % change in the initial (root zone) soil moisture S_s. The sensitivity range given relates to the minimum and maximum sensitivities for an initial soil moisture range between 0% and 90% as of Fig. 9.

Catchment	Giofiros	Almirida	Rastenberg	Rastenberg
Catchment area (km^2)	186.7	24.7	96.0	96.0
Mean annual precipitation (mm)	827	648	900	900
Event	13th Jan. 1994	17th Oct. 2006	7th Aug. 2000	7th Aug. 2002
Event precipitation (mm)	183	220	23	200
Initial soil moisture (%)	22	2.5	36	51
Peak flow (m^3/s)	296	123.5	2.5	110
Specific peak flow ($m^3/s/km^2$)	1.59	5.00	0.03	1.15
Sensitivity (% flood peak change per % soil moisture change)	0.51–0.88	0.18–0.25	0.42–3.39	0.21–0.92

It is also interesting to note that the non-linearity in the smaller floods is larger than it is for the larger floods. This is consistent with the hydrological reasoning of the role of initial losses. (Vieux et al., 2009) notes that "The sensitivity of the watershed response to the initial degree of saturation is dependent on event magnitude but becomes increasingly sensitive at higher degrees of initial saturation." This is exactly what has been found in the present analysis for the Rastenberg events. The non-linearity is mainly due to the high permeability of the sandy soils that fill up and spill over like a bucket (Komma et al., 2008, 2007). It is also interesting to note that the differences between the climates (Mediterranean climate in Crete as opposed to a more continental climate in Austria) seem to affect the sensitivity of flood peaks to initial soil moisture less than the precipitation event magnitude. While the moisture range can be larger in the Mediterranean catchments, climate does not seem to be the main control on flood response sensitivity for the events examined in this paper.

A sensitivity of up to 3% flood peak change per % soil moisture change looks large as, depending on whether the soil is wet or dry the runoff peak may more than double. It should be noted that, in the sensitivity analysis of this paper, the root zone soil moisture S_s was varied while the remaining moisture storage in the aquifers was assumed to be unchanged. This was to understand the accuracy of satellite based soil moisture estimates needed for water hazard forecasts. If the entire catchment (including aquifers) dries out or wets up, the sensitivities can be even larger than those found in this paper, particularly for small events.

The coefficients of determination obtained by comparing the SWI to catchment scale simulated soil moisture ranged from 0.37 in the Rastenberg catchment to 0.82 in the Giofiros catchment. The Rastenberg r^2 is relatively low because of the forest cover and the influence of snow in the catchment while Giofiros is essentially unforested and there is no snow. For the latter types of catchments one can expect excellent correlations between the

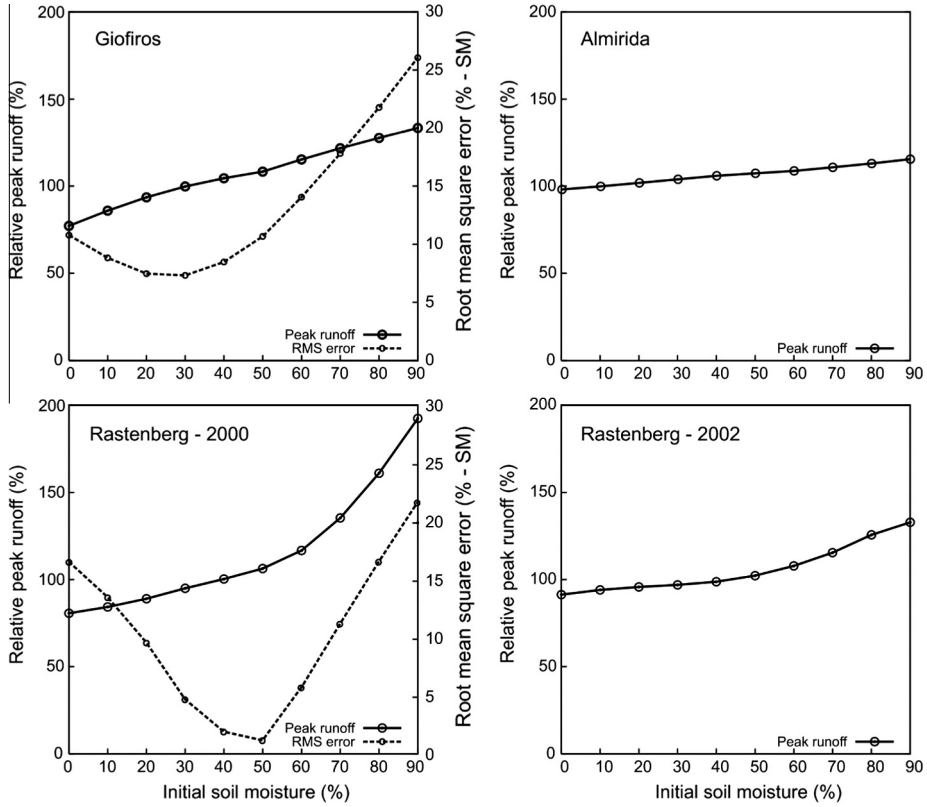

Fig. 10. Initial soil moisture (S_s) effect on relative peak discharge (peak runoff of the sensitivity study divided by observed peak runoff in % – solid line) and RMS error between simulated soil moisture (S_s) and SWI index values for the event simulation periods (dashed line). The upper panels show the Crete catchments Giofiros and Almirida, the lower panels show the 2000 and the 2002 events of the Rastenberg catchment in Austria.

scatterometer SWI and soil moisture simulated by a hydrological model which may be better than those between the scatterometer SWI and point soil moisture measurements (Western et al., 2002). It appears that the small scale variability of soil moisture and scale issues confound the comparability of the point measurements with the scatterometer SWI which applies to space scales of hundreds of km^2 (Western et al., 2002). This makes it difficult to find relationships across scales (Blöschl, 2006). In contrast, the catchment scale hydrological model simulations seem to be fairly consistent with the SWI index.

The analysis of all events suggests that the scatterometer SWI can give valuable information for flash flood forecasting and, more generally, flood hazard assessments. Obviously, the value of the scatterometer data depends on how well it actually represents catchment soil moisture and on the amount of hydrological ground data available. For sparse hydrological networks, the scatterometer soil moisture may be more important than for well instrumented catchments. The results in this paper indicate that the effect of initial soil moisture on the flood magnitudes depends on event magnitude and to a lesser degree on climate or region. The type of the soil also plays an important role to the response of the runoff. In the Rastenberg catchment the deep, sandy soils are the main reasons for the non-linear runoff response behaviour and are strongly related to the soil moisture dynamics in the catchment. In contrast, the shallow and relatively more impermeable soils of Cretan case studies describe well the more linear relationship between the flood peak and the initial soil moisture. However, it should be noted that only four events have been examined. While three of these events were very large and therefore of particular interest to flash flood warning, an extension of the present study to a larger number of catchments and events would be of interest.

Given the importance of initial soil moisture on flood generation, the use of soil moisture satellite data seems to be a logical way forward to contribute to more reliable flash flood warnings. This can be either done by assimilating soil moisture into hydrological forecasting systems (Parajka et al., 2009, 2006; Wanders et al., 2014) or by combining flash flood guidance based on rainfall depth-duration thresholds (Norbiato et al., 2009) with satellite estimates of soil moisture.

References

Apel, H., Thieken, A.H., Merz, B., Blöschl, G., 2006. A probabilistic modelling system for assessing flood risks. Nat. Hazards 38, 79–100. http://dx.doi.org/10.1007/s11069-005-8603-7.

Apel, H., Thieken, A.H., Merz, B., Blöschl, G., 2004. Flood risk assessment and associated uncertainty. Nat. Hazards Earth Syst. Sci. 4, 295–308. http://dx.doi.org/10.5194/nhess-4-295-2004.

Bartalis, Z., Scipal, K., Wagner, W., 2006. Azimuthal anisotropy of scatterometer measurements over land. IEEE Trans. Geosci. Rem. Sens. 44, 2083–2092. http://dx.doi.org/10.1109/TGRS.2006.872084.

Bartalis, Z., Wagner, W., Naeimi, V., Hasenauer, S., Scipal, K., Bonekamp, H., Figa, J., Anderson, C., 2007. Initial soil moisture retrievals from the METOP – a advanced scatterometer (ASCAT). Geophys. Res. Lett. 34, L20401. http://dx.doi.org/10.1029/2007GL031088.

Berthet, L., Andréassian, V., Perrin, C., Javelle, P., 2009. How crucial is it to account for the antecedent moisture conditions in flood forecasting? Comparison of event-based and continuous approaches on 178 catchments. Hydrol. Earth Syst. Sci. 13, 819–831. http://dx.doi.org/10.5194/hess-13-819-2009.

Blöschl, G., 2010. Flood warning – on the value of local information. Int. J. River Basin Manag.

Blöschl, G., 2006. Hydrologic synthesis: across processes, places, and scales. Water Resour. Res. 42. http://dx.doi.org/10.1029/2005WR004319, n/a–n/a.

Bloschl, G., Reszler, C., Komma, J., 2008. A spatially distributed flash flood forecasting model. Environ. Model. Softw. 23, 464–478. http://dx.doi.org/10.1016/j.envsoft.2007.06.010.

Brocca, L., Melone, F., Moramarco, T., Wagner, W., Naeimi, V., Bartalis, Z., Hasenauer, S., 2010. Improving runoff prediction through the assimilation of the ASCAT soil moisture product. Hydrol. Earth Syst. Sci. 14, 1881–1893. http://dx.doi.org/10.5194/hess-14-1881-2010.

Brocca, L., Moramarco, T., Melone, F., Wagner, W., Hasenauer, S., Hahn, S., 2012. Assimilation of surface- and root-zone ASCAT soil moisture products into rainfall–runoff modeling. IEEE Trans. Geosci. Rem. Sens. 50, 2542–2555. http://dx.doi.org/10.1109/TGRS.2011.2177468.

Daliakopoulos, I.N., Tsanis, I.K., 2012. A weather radar data processing module for storm analysis. J. Hydroinfor. 14, 332. http://dx.doi.org/10.2166/hydro.2011.118.

de Jeu, R.A.M., Wagner, W., Holmes, T.R.H., Dolman, A.J., van de Giesen, N.C., Friesen, J., 2008. Global soil moisture patterns observed by space borne microwave radiometers and scatterometers. Surv. Geophys. 29, 399–420. http://dx.doi.org/10.1007/s10712-008-9044-0.

Ganoulis, J., 2003. Risk-based floodplain management: a case study from Greece. Int. J. River Basin Manag. 1, 41–47. http://dx.doi.org/10.1080/15715124.2003.9635191.

Gaume, E., Bain, V., Bernardara, P., Newinger, O., Barbuc, M., Bateman, A., Blaškovičová, L., Blöschl, G., Borga, M., Dumitrescu, A., Daliakopoulos, I., Garcia, J., Irimescu, A., Kohnova, S., Koutroulis, A., Marchi, L., Matreata, S., Medina, V., Preciso, E., Sempere-Torres, D., Stancalie, G., Szolgay, J., Tsanis, I., Velasco, D., Viglione, A., 2009. A compilation of data on European flash floods. J. Hydrol. 367, 70–78. http://dx.doi.org/10.1016/j.jhydrol.2008.12.028.

Georgakakos, K.P., 2006. Analytical results for operational flash flood guidance. J. Hydrol. 317, 81–103. http://dx.doi.org/10.1016/j.jhydrol.2005.05.009.

Grayson, R., Blöschl, G., 2001. Spatial patterns in catchment hydrology: observations and modelling. CUP Arch.

Grayson, R.B., Western, A.W., Chiew, F.H.S., Blöschl, G., 1997. Preferred states in spatial soil moisture patterns: local and nonlocal controls. Water Resour. Res. 33, 2897–2908. http://dx.doi.org/10.1029/97WR02174.

Grillakis, M.G., Tsanis, I.K., Koutroulis, A.G., 2010. Application of the HBV hydrological model in a flash flood case in Slovenia. Nat. Hazards Earth Syst. Sci. 10, 2713–2725. http://dx.doi.org/10.5194/nhess-10-2713-2010.

Hall, J., Arheimer, B., Borga, M., Brázdil, R., Claps, P., Kiss, A., Kjeldsen, T.R., Kriauciuniene, J., Kundzewicz, Z.W., Lang, M., Llasat, M.C., Macdonald, N., Mcintyre, N., Mediero, L., Merz, B., Merz, R., Molnar, P., Montanari, A., Neuhold, C., Parajka, J., Perdigão, R.A.P., Plavcová, L., Rogger, M., Salinas, J.L., Sauquet, E., Schär, C., Szolgay, J., Viglione, A., Blöschl, G., 2013. Understanding flood regime changes in Europe: a state of the art assessment. Hydrol. Earth Syst. Sci. Discuss. 10, 15525–15624.

Hlavcova, H., Kohnova, S., Kubes, R., Szolgay, J., Zvolensky, M., 2005. An empirical method for estimating future flood risks for flood warnings. Hydrol. Earth Syst. Sci. Discuss. 9, 431–448.

Javelle, P., Fouchier, C., Arnaud, P., Lavabre, J., 2010. Flash flood warning at ungauged locations using radar rainfall and antecedent soil moisture estimations. J. Hydrol. 394, 267–274. http://dx.doi.org/10.1016/j.jhydrol.2010.03.032.

Joshi, C., Mohanty, B.P., Jacobs, J.M., Ines, A.V.M., 2011. Spatiotemporal analyses of soil moisture from point to footprint scale in two different hydroclimatic regions. Water Resour. Res. 47. http://dx.doi.org/10.1029/2009WR009002, n/a–n/a.

Komma, J., Blöschl, G., Reszler, C., 2008. Soil moisture updating by Ensemble Kalman Filtering in real-time flood forecasting. J. Hydrol. 357, 228–242. http://dx.doi.org/10.1016/j.jhydrol.2008.05.020.

Komma, J., Reszler, C., Blöschl, G., Haiden, T., 2007. Ensemble prediction of floods – catchment non-linearity and forecast probabilities. Nat. Hazards Earth Syst. Sci. 7, 431–444. http://dx.doi.org/10.5194/nhess-7-431-2007.

Koutroulis, A.G., Tsanis, I.K., 2010. A method for estimating flash flood peak discharge in a poorly gauged basin: case study for the 13–14 January 1994 flood, Giofiros basin, Crete, Greece. J. Hydrol. 385, 150–164. http://dx.doi.org/10.1016/j.jhydrol.2010.02.012.

Lacava, T., Greco, M., Di Leo, E.V., Martino, G., Pergola, N., Sannazzaro, F., Tramutoli, V., 2005. Monitoring soil wetness variations by means of satellite passive microwave observations: the HYDROPTIMET study cases. Nat. Hazards Earth Syst. Sci. 5, 583–592. http://dx.doi.org/10.5194/nhess-5-583-2005.

Lagouvardos, K., Kotroni, V., Nickovic, S., Kallos, G., 1996. Evidence of a winter tropical storm over eastern Mediterranean: simulations with the regional atmospheric modelling system (RAMS) and the ETA/NMC model. In: 7th International Conference on Mesoscale Processes.

Merz, B., Thieken, A.H., 2009. Flood risk curves and uncertainty bounds. Nat. Hazards 51, 437–458. http://dx.doi.org/10.1007/s11069-009-9452-6.

Merz, R., Blöschl, G., 2008a. Flood frequency hydrology: 1. Temporal, spatial, and causal expansion of information. Water Resour. Res. 44. http://dx.doi.org/10.1029/2007WR006744, n/a–n/a.

Merz, R., Blöschl, G., 2008b. Flood frequency hydrology: 2. Combining data evidence. Water Resour. Res. 44. http://dx.doi.org/10.1029/2007WR006745, n/a–n/a.

Michele, C.D., Salvadori, G., 2002. On the derived flood frequency distribution: analytical formulation and the influence of antecedent soil moisture condition. J. Hydrol. 262, 245–258. http://dx.doi.org/10.1016/S0022-1694(02)00025-2.

Naeimi, V., Scipal, K., Bartalis, Z., Hasenauer, S., Wagner, W., 2009. An improved soil moisture retrieval algorithm for ERS and METOP scatterometer observations. IEEE Trans. Geosci. Rem. Sens. 47, 1999–2013. http://dx.doi.org/10.1109/TGRS.2008.2011617.

Nasta, P., Sica, B., Chirico, G.B., Ferraris, S., Romano, N., 2013. Analysis of near-surface soil moisture spatial and temporal dynamics in an experimental catchment in Southern Italy. Proc. Environ. Sci. 19, 188–197. http://dx.doi.org/10.1016/j.proenv.2013.06.021.

Norbiato, D., Borga, M., Dinale, R., 2009. Flash flood warning in ungauged basins by use of the flash flood guidance and model-based runoff thresholds. Meteorol. Appl. 16, 65–75. http://dx.doi.org/10.1002/met.126.

Parajka, J., Naeimi, V., Blöschl, G., Komma, J., 2009. Matching ERS scatterometer based soil moisture patterns with simulations of a conceptual dual layer

hydrologic model over Austria. Hydrol. Earth Syst. Sci. 13, 259–271. http://dx.doi.org/10.5194/hess-13-259-2009.
Parajka, J., Naeimi, V., Blöschl, G., Wagner, W., Merz, R., Scipal, K., 2006. Assimilating scatterometer soil moisture data into conceptual hydrologic models at the regional scale. Hydrol. Earth Syst. Sci. 10, 353–368. http://dx.doi.org/10.5194/hess-10-353-2006.
Peel, M.C., Finlayson, B.L., McMahon, T.A., 2007. Updated world map of the Köppen-Geiger climate classification. Hydrol. Earth Syst. Sci. 11, 1633–1644. http://dx.doi.org/10.5194/hess-11-1633-2007.
Raynaud, D., Thielen, J., Salamon, P., Burek, P., Anquetin, S., Alfieri, L., 2015. A dynamic runoff co-efficient to improve flash flood early warning in Europe: evaluation on the 2013 central European floods in Germany. Meteorol. Appl. 22, 410–418. http://dx.doi.org/10.1002/met.1469.
Reszler, C., Komma, J., Blöschl, G., Gutknecht, D., 2008. Dominante Prozesse und Ereignistypen zur Plausibilisierung flächendetaillierter Niederschlag-Abflussmodelle. Hydrol. und Wasserbewirtschaftung 52, 120–131.
Tsanis, I.K., Seiradakis, K.D., Daliakopoulos, I.N., Grillakis, M.G., Koutroulis, A.G., 2013. Assessment of Geoeye-1 stereo-pair generated DEM in flood mapping of an ungauged basin. J. Hydroinf. 16 (1), 1–18.
Van Steenbergen, N., Willems, P., 2013. Increasing river flood preparedness by real-time warning based on wetness state conditions. J. Hydrol. 489, 227–237. http://dx.doi.org/10.1016/j.jhydrol.2013.03.015.
Vieux, B.E., Park, J.-H., Kang, B., 2009. Distributed hydrologic prediction: sensitivity to accuracy of initial soil moisture conditions and radar rainfall input. J. Hydrol. Eng. 14, 671–689. http://dx.doi.org/10.1061/(ASCE)HE.1943-5584.0000039.
Viglione, A., Chirico, G.B., Komma, J., Woods, R., Borga, M., Blöschl, G., 2010. Quantifying space-time dynamics of flood event types. J. Hydrol. 394, 213–229. http://dx.doi.org/10.1016/j.jhydrol.2010.05.041.
Viglione, A., Merz, R., Blöschl, G., 2009. On the role of the runoff coefficient in the mapping of rainfall to flood return periods. Hydrol. Earth Syst. Sci. 13, 577–593. http://dx.doi.org/10.5194/hess-13-577-2009.
Wagner, W., 1998. Soil Moisture Retrieval from ERS Scatterometer Data. Vienna University of Technology.
Wagner, W., Lemoine, G., Rott, H., 1999. A method for estimating soil moisture from ERS scatterometer and soil data. Rem. Sens. Environ. 70, 191–207. http://dx.doi.org/10.1016/S0034-4257(99)00036-X.
Wanders, N., Karssenberg, D., de Roo, A., de Jong, S.M., Bierkens, M.F.P., 2014. The suitability of remotely sensed soil moisture for improving operational flood forecasting. Hydrol. Earth Syst. Sci. 18, 2343–2357. http://dx.doi.org/10.5194/hess-18-2343-2014.
Western, A.W., Grayson, R.B., Blöschl, G., 2002. Scaling of soil moisture: a hydrologic perspective. Annu. Rev. Earth Planet. Sci. 30, 149–180. http://dx.doi.org/10.1146/annurev.earth.30.091201.140434.
Yatheendradas, S., Wagener, T., Gupta, H., Unkrich, C., Goodrich, D., Schaffner, M., Stewart, A., 2008. Understanding uncertainty in distributed flash flood forecasting for semiarid regions. Water Resour. Res. 44, 91–92. http://dx.doi.org/10.1029/2007WR005940, n/a–n/a.
Yoo, C., Valdés, J.B., North, G.R., 1998. Evaluation of the impact of rainfall on soil moisture variability. Adv. Water Resour. 21, 375–384. http://dx.doi.org/10.1016/S0309-1708(97)00002-X.
Zehe, E., Blöschl, G., 2004. Predictability of hydrologic response at the plot and catchment scales: role of initial conditions. Water Resour. Res. 40. http://dx.doi.org/10.1029/2003WR002869, n/a–n/a.